Temperature dependence of the Casimir-like force in free-standing smectic films

I. N. de Oliveira,[1] M. L. Lyra,[1] and L. V. Mirantsev[2]
[1]*Instituto de Física, Universidade Federal de Alagoas, 57072-970 Maceió-Alagoas, Brazil*
[2]*Institute of the Problems of Mechanical Engineering, Academy of Sciences of Russia, 199178 St. Petersburg, Russia*
(Received 19 September 2005; published 6 April 2006)

The thermal Casimir-like force in free-standing liquid crystal films close to the smectic-*A*–nematic transition temperature is computed using a quadratic functional approach. In the framework of a microscopic mean-field model of free-standing smectic-*A* films, the temperature dependence of the order parameter profiles is computed and later used to estimate the elastic coupling variability in the vicinity of first- and second-order bulk smectic-*A*–nematic phase transitions. The strong nonuniformity of the coupling constant profiles promotes a significant increase of the fluctuation-induced force over three orders of magnitude, especially in thin films. This result reinforces the possible predominance of the thermal Casimir force as compared to the standard van der Waals interaction in thin smectic-*A* liquid crystal films.

DOI: 10.1103/PhysRevE.73.041703 PACS number(s): 61.30.Cz, 61.30.Hn, 61.30.Dk, 64.70.Md

I. INTRODUCTION

A unique property of smectic liquid crystals is the ability to form free-standing smectic films (FSSF's) which can be considered as a stack of smectic layers confined by a surrounding gas [1,2]. The combination of surface-induced ordering and finite-size effects in FSSF's gives rise to a series of phenomena that are not observed in bulk liquid crystal (LC) samples. These phenomena are the existence of smectic films at high temperatures as compared with bulk samples [3,4], surface-enhanced ordering, and layer-thinning transitions [5–7]. Due to their unusual properties, FSSF's are objects of intensive experimental and theoretical investigations.

Thermal fluctuations in FSSF's with slowly decaying (power-law) correlations produce a fluctuation-induced long-range interaction between the film surfaces [8–14]. Usually, this thermal Casimir-like force has a longer range than the van der Waals interaction and can be expected to play a relevant role in governing the behavior of FSSF's. In particular, the Casimir-like smectic force is predicted to be predominant over the van der Waals interaction in phenomena in which the smectic fluctuation profile is nonuniform, such as wetting and layer-thinning transitions [15–18]. On the other hand, in cases where the fluctuation profile is uniform, like layer-by-layer freezing [19], the Casimir-like force has a faster decay than the van der Waals interaction [12,20].

In previous work [20,21], the surface effects and field-driven crossover in the Casimir-like force were examined in FSSF's of thickness ℓ. In particular, it has been shown that, due to ordering field terms, the typical $1/\ell$ decay of the fluctuation-induced surface-surface interaction energy is replaced by a faster $1/\ell^2$ decay. The main results were derived within the framework of Holyst's model [22,23] for thermal fluctuations in free-standing smectic-*A* films (FSSAF's). In the Holyst model, the FSSAF elastic properties are assumed to be spatially uniform and characterized by the bending elastic constant K and the compressibility of the smectic layers B which are set similar for all film layers and equal to those at the bulk smectic-*A* (Sm*A*) phase. This assumption is physically justified for FSSAF's well below the bulk smectic-*A*–isotropic (Sm*A*-*I*) or smectic-A–nematic (Sm*A*-*N*) transition temperatures when the smectic order is well developed in the whole volume of the film.

However, FSSAF's can exist at temperatures significantly higher than the bulk phase transition temperature. According to a microscopic model [24,25], which describes many features of FSSAF's at temperatures well above the bulk Sm*A*-*I* or Sm*A*-*N* transitions, the internal film layers can be less ordered than the outermost ones. Therefore, the orientational s and translational σ order parameters for smectic layers situated far from the boundary surfaces of the film can be smaller than those for the outermost film layers and this nonuniformity of the film should be taken into account when the Casimir-like force is computed. Of course, in such presmectic films, the so-called structural forces are usually large enough to mask the Casimir force [26,27]. However, the nonuniformity of the order parameter profiles persists even for temperatures slightly below the bulk transition temperature. In this situation, the structural forces are expected to be very weak and the Casimir-like contribution to the surface-surface effective interaction may become predominant.

It is well known that, in macroscopic bulk LC samples, the elastic constants K and B are proportional to s^2 and σ^2, respectively [1,2]. Although the smectic film layers have a microscopic thickness comparable to the molecular length l^*, their length and width are macroscopic. Hence, each film layer can be considered as a macroscopic ensemble, consisting of a very large number of molecules, over which one can perform the same statistical-mechanical average of physical values, such as order parameters s and σ, and elastic couplings K and B, as in the case of the macroscopic bulk LC samples. As a result, we can assume that, for the smectic film layers, the relation between the elastic couplings K and B and order parameters s^2 and σ^2, respectively, should be similar to analogous relations for macroscopic bulk LC samples. Therefore, the values of the elastic couplings K and B for interior film layers should be significantly smaller than those near the boundary surfaces of the FSSAF.

Using a microscopic model [24,25], one of us extended the Holyst model for FSSAF's by taking into account these

 ©2006 The American Physical Society

nonuniform elastic constant profiles [28,29]. Close to bulk Sm*A*-*I* or Sm*A*-*N* transition temperatures, this approach showed that these profiles have a significant effect on thermal fluctuations and such a feature points toward a strong influence of the nonuniformity of the elastic couplings on the fluctuation-induced Casimir-like interaction between the free surfaces of smectic films.

The present paper is devoted to the investigation of the influence of the elastic constant profile nonuniformities on the Casimir-like force in free-standing smectic-*A* films within a Gaussian functional integral approach. The profiles of the elastic constants K and B are numerically computed from the microscopic model of FSSAF's [24,25]. We will show that, close to the bulk first- and second-order Sm*A*-*N* phase transition temperatures, the amplitude of the Casimir-like force has a strong dependence on the order parameter profiles. In both cases, the amplitude of the Casimir-like force grows for several orders of magnitude when the temperature approaches the transition temperature, thus indicating that the thermal Casimir-like contribution due to the smectic layer displacement fluctuations predominates over the van der Waals force. Also, the nonuniformity of the K and B profiles in the vicinity of the bulk transition temperature modifies the dependence of the Casimir-like force on the film thickness ℓ. Close to the second-order bulk Sm*A*-*N* transition temperature, the force decays with the thickness l as $1/\ell^{3/2}$ in contrast to the $1/\ell^2$ decay far from the transition point. This feature is due to the divergence of the typical correlation length which also governs the vanishing of the compressibility constant B.

II. MODEL

In the harmonic approximation, the fluctuation Hamiltonian for a thin free-standing smectic-*A* film with N layers can be written as

$$H=\int_a^L d^2r\left[\sum_{i=1}^{N}\frac{dK_i}{2}[\Delta u_i(\mathbf{r})]^2+\sum_{i=1}^{N-1}\left(\frac{B_i+B_{i+1}}{4d}\right)\times[u_{i+1}(\mathbf{r})-u_i(\mathbf{r})]^2+\frac{\gamma}{2}|\nabla u_1(\mathbf{r})|^2+\frac{\gamma}{2}|\nabla u_N(\mathbf{r})|^2\right], \quad (1)$$

where $u_i(\mathbf{r})$ is the ith-layer displacement from its original equilibrium position at $z=id$. Here, d is the average distance between layers, L is the transversal size of the film, and a is a short-wavelength in-layer cutoff of the order of the short molecular axis. The above Hamiltonian therefore describes a system composed of a finite number of coupled continuous layers. All thermodynamic course-grained quantities are independent of the in-layer cutoff. K_i and B_i stand for the bending and compressibility elastic constants of the ith layer, respectively, γ is the surface tension which represents the additional energy cost associated with variations on the area of the free surfaces, with the equilibrium direction being determined by the holder used in the free-standing film technique [30]. A characteristic surface tension $\gamma_c=\sqrt{KB}$ delimits the regimes of strong ($\gamma>\gamma_c$) and weak surface tension ($\gamma<\gamma_c$). Here, K and B are the bulk elastic constants which are temperature dependent [1,2]. Recent works have shown that the surface tension also depends on the temperature and film thickness [31–33]. However, its temperature dependence near the first- and second-order Sm*A*-*N* phase transitions is less pronounced as compared with K and B, and variations of the surface tension γ can be neglected [34,35]. As said above, this model was originally introduced by Holyst [22,23] to investigate the x-ray diffraction for thin smectic-*A* films and further extended by Mirantsev [28,29] to compute thermal properties of films taking into account nonuniform elastic constant profiles.

Taking the continuous Fourier transform with respect to $\mathbf{r}$, one can write the Hamiltonian (1) in the more compact form

$$H=\frac{1}{2}\int_{2\pi/L}^{2\pi/a}\frac{d^2q}{(2\pi)^2}\sum_{i,j}u_i(q)M_{ij}u_j(-q), \quad (2)$$

where the nonzero elements of the interaction matrix $\mathbf{M}$ are

$$M_{1,1}=K_1dq^4+\gamma q^2+(B_1+B_2)/2d, \quad (3)$$

$$M_{i,i}=K_idq^4+(B_{i-1}+2B_i+B_{i+1})/2d, \quad i=2,\ldots,N-1 \quad (4)$$

$$M_{N,N}=K_Ndq^4+\gamma q^2+(B_{N-1}+B_N)/2d, \quad (5)$$

$$M_{i,i+1}=M_{i+1,i}=-(B_i+B_{i+1})/2d, \quad i=1,\ldots,N-1. \quad (6)$$

The quadratic form (2) of the Hamiltonian allows to perform the analytical computation of some thermodynamic quantities. In particular, the total free energy per unit area of the film is given by

$$\frac{f}{k_BT}=\frac{1}{2}\int_{2\pi/L}^{2\pi/a}\frac{d^2q}{(2\pi)^2}\ln(\det M). \quad (7)$$

This total free energy has the following functional dependence on the film thickness ℓ:

$$f=f_B+f_S+\Delta f(\ell), \quad (8)$$

where f_B and f_S are the bulk and surface contributions to the total free energy, respectively. The last term $\Delta f(\ell)$ is the effective surface-surface interaction energy due to the smectic layer displacement fluctuations. In models which consider the film continuous also in the direction perpendicular to the layers, the volume and surface contributions to the free energy are formally divergent. In such case, a regularization procedure is needed to separate them from the fluctuation-induced contribution. The regularization schemes usually introduce a perpendicular cutoff to make these contributions finite with the remaining thermodynamic quantities being cutoff independent. In the present model of a smectic film with discrete layers, the volume and surface contributions are finite. Hence no further regularization is needed once the layer spacing already acts as a natural cutoff perpendicular to the layers plane. We can split numerically the Casimir-like contribution making use of the functional dependence of the different terms on the film thickness. The volume contribution is obtained using an auxiliary thick film with uniform

bulk couplings and periodic boundary conditions. The Casimir-like force is obtained after subtracting the remaining free energy of ℓ-layer and $(\ell+1)$-layer films, respectively.

Earlier results have shown that the Casimir-like force is strongly influenced by the shape of the smectic fluctuation profile [20,21]. Here, we are interested in computing the temperature dependence of the smectic thermal Casimir force due to the variability of the elastic constants. Their profiles can be obtained from the orientational s_i and translational σ_i order parameters of each film layer. These parameters can be computed, within a mean-field approach, from a recently introduced extended McMillan model [24,25]. In this model, the one-particle effective potential within a smectic layer is given by

$$V_1(z_1,\theta_1) = -\frac{V_0}{3}[s_1 + s_2 + 3W_0/V_0 + \alpha\cos(2\pi z_1/d)(\sigma_1+\sigma_2)]P_2(\cos\theta_1), \quad (9)$$

$$V_i(z_i,\theta_i) = -\frac{V_0}{3}\left[\sum_{i-1}^{i+1} s_i + \alpha\cos(2\pi z_i/d)\left(\sum_{i-1}^{i+1}\sigma_i\right)\right]P_2(\cos\theta_i), \quad (10)$$

$$V_N(z_N,\theta_N) = -\frac{V_0}{3}[s_N + s_{N-1} + 3W_0/V_0 + \alpha\cos(2\pi z_N/d)(\sigma_N+\sigma_{N-1})]P_2(\cos\theta_N). \quad (11)$$

Here, $P_2(\cos\theta_i)$ is the second-order Legendre polynomial with θ_i being the angle in the ith layer between the long axis of the molecule and the z direction. V_0 is a parameter of the microscopic model [36] that determines the scale of the nematic-isotropic transition temperature. The parameter α is related to the length of alkyl tails of calamitic molecules through the well-known relation $\alpha=2\exp[-(r_0/l^*)^2]$, where r_0 is the characteristic length of the model intermolecular interaction, and the molecular length l^* is proportional to that of the alkyl tails.

In the microscopic mean-field model for finite films [24,25], the strength of surface anchoring is determined by the parameter W_0. This parameter couples with orientational order parameter s and represents the surface-induced homeotropic alignment in the film. In FSSAF's, the absence of a substrate gives rise to an almost perfect homeotropic alignment at the film surfaces [37]. We will assume that, for the ith layer, the bending elastic modulus K_i is proportional to s_i^2 and the compressibility modulus is proportional to σ_i^2 [28,29]. For thick films $(N\to\infty)$ the local order parameters should have values predicted by McMillan theory [36] for the bulk SmA phase. At the temperature T_0 well below the bulk SmA-N transition temperature, we can assume the bulk order parameters to be s_0 and σ_0 and set the corresponding elastic constants $K(T_0)=K_0$ and $B(T_0)=B_0$. Knowing values of B_0 and K_0 at the reference temperature T_0, we can obtain the elastic constant profiles at temperature T using the following expressions:

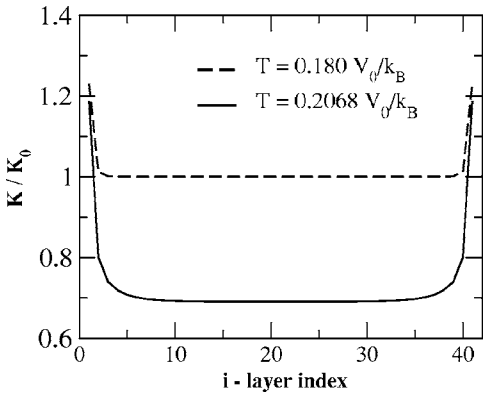

FIG. 1. Normalized bending elastic constant versus layer index for a 41-layer FSSAF at distinct temperatures. The bulk transition temperature is $T_{AN}=0.206\,988V_0/k_B$. The parameters of the microscopic model [24,25] are $W_0=1.8V_0$ and $\alpha=0.85$.

$$K_i(T) = K_0\left(\frac{s_i(T)}{s_0}\right)^2, \quad (12)$$

$$B_i(T) = B_0\left(\frac{\sigma_i(T)}{\sigma_0}\right)^2. \quad (13)$$

The elastic constant profiles may have distinct behaviors near the first- and second-order phase transitions depending on the order parameter profiles. The order of the bulk phase transition is determined by the parameter α. McMillan theory [36] predicts that for $\alpha<0.7$ the bulk SmA-N transition is continuous, i.e., the smectic order parameter vanishes continuously as one approach the transition temperature. For $0.7<\alpha<0.98$ the SmA-N transition is a first-order one, with the smectic order parameter changing abruptly from a finite value to zero when crossing the transition temperature. For values of α above 0.98, a first-order SmA-I phase transition takes place. We will consider values of α that correspond to SmA-N transitions. In particular, we will use $\alpha=0.85$ (for which the bulk SmA-N first-order transition temperature is $T_{AN}=0.206\,988V_0/k_B$), and $\alpha=0.6$ (for which the bulk second-order transition temperature is $T_{AN}=0.177\,261V_0/k_B$). We performed our calculations using $W_0=1.8V_0$ which corresponds to a strong homeotropic anchoring at the free surfaces of the film. In what follows, we use as reference temperatures $T_0=0.150V_0/k_B$ for $\alpha=0.6$ and $T_0=0.180V_0/k_B$ for $\alpha=0.85$, which are well below the transition temperature in either case. At these temperatures, we considered the elastic constants having typical values, namely, $B_0=10^8$ dyn/cm^2 and $K_0=10^{-6}$ dyn.

III. RESULTS OF COMPUTATION

In Fig. 1, we show the bending elastic constant versus layer index i of a 41-layer film at distinct temperatures. In this case, $\alpha=0.85$, corresponding to a bulk first-order SmA-N transition. At the reference temperature, which is well below the bulk transition temperature, the bending constant profile is uniform in the whole film except at the outermost film layers. Close to the bulk transition temperature,

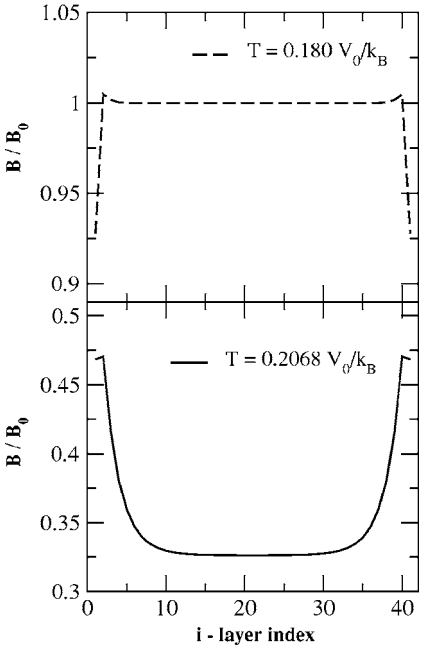

FIG. 2. Normalized compressibility elastic constant versus layer index for a 41-layer film at distinct temperatures. The parameters are the same as in Fig. 1.

the nonuniform feature of the profile is more pronounced, but the bending constant profile of inner layers is still flat. In Fig. 2, we show the compressibility elastic constant as a function of the layer index for the same film at distinct temperatures. Again, at the reference temperature the profile is uniform except at the surface layers. Close to the phase transition, there is a pronounced reduction in the value of the compressibility constant and the profile becomes nonuniform over a longer distance to the film surface. For both compressibility and bending constants, the surface effects are more pronounced for thinner films for which the order parameter profiles become strongly nonuniform near the transition temperature.

For temperatures not very close to the Sm*A*-*N* transition temperature, the compressibility of the outermost film layers is slightly smaller than that of other film layers. To understand this feature, once should notice that, according to the microscopic mean-field model [24,25], an orienting action of the boundary surfaces on the LC molecules of the film is simulated by a short range orienting field, which acts directly only on molecules within the first and last outermost film layers. This field enhances the orientational order in these layers and such enhancement is transmitted to the next film layers. Since the nematic and smectic orders are connected to each other, the smectic order is also enhanced in the layers adjoined to the outermost ones. However, when the temperature of the film is significantly lower than the bulk smectic-*A* to nematic transition temperature for which the smectic order is well developed in the whole volume of the film, this enhancement is very small. In this case, the smectic order in the outermost film layers can be even slightly lower than that in the interior ones because molecules of the outermost layers interact directly with molecules of only a single neighboring layer whereas molecules of each interior film layer interact

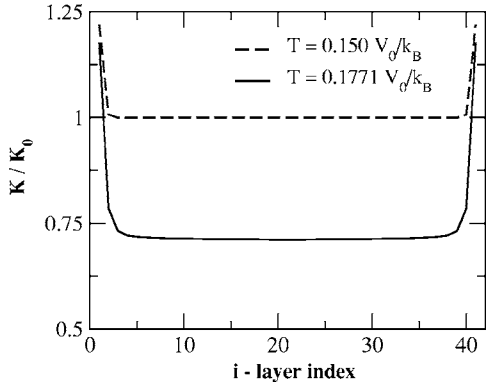

FIG. 3. Normalized bending elastic constant versus layer index for films at distinct temperatures. The bulk transition temperature is $T_{AN}=0.177\,261V_0/k_B$. The model parameters are $W_0=1.8V_0$ and $\alpha=0.6$.

with molecules of two neighboring layers. Therefore, the compressibility of the subsurface smectic layers becomes smaller than that of the interior film layers. On the contrary, when the temperature of the film is very close to the bulk smectic-*A* to nematic transition temperature and the smectic order is weakened in the interior film layers, the orienting action of the boundary surfaces of the film on the LC molecules of the outermost film layers gives rise to an enhancement of the smectic order in the interfacial film layers as compared to smectic order in the interior ones. Hence, the compressibility of the subsurface smectic layers is higher than that of the interior film layers.

Taking $\alpha=0.6$, corresponding to a second-order Sm*A*-*N* transition, we obtain bending and compressibility profiles exhibiting distinct trends. In Fig. 3, we plot the bending elastic constant as a function of the layer index both for the reference temperature and close to the bulk transition temperature for a 41-layer film. The bending profiles exhibit a behavior quite similar to that observed in the case of a first order Sm*A*-*N* transition with inner layers keeping a uniform profile. On the other hand, the compressibility profiles have a quite different behavior in this case. At the reference temperature, the compressibility profile has a negative concavity and is uniform for inner layers, as shown in Fig. 4. Close to the transition temperature, the compressibility profile exhibits a positive concavity with a significant reduction of magnitude. Such reduction reflects the vanishing of the translational order parameter in the case of the second-order phase transition. Also, the compressibility profile is nonuniform in the whole film.

The nonuniform feature of the elastic constant profiles close to first- and second-order phase transitions can induce a significant temperature dependence of the Casimir-like force. This fluctuation-induced force per unit area for films with uniform elastic constant profiles has an asymptotic functional dependence given by

$$\frac{F}{k_BT}=-\frac{\Delta(T)}{\lambda_c}\left(\frac{1}{\ell}\right)^2, \tag{14}$$

with $\ell=Nd$. In the continuous limit, it is straightforward to show that the asymptotic amplitude $\Delta(T)$ can be written as [8,20]

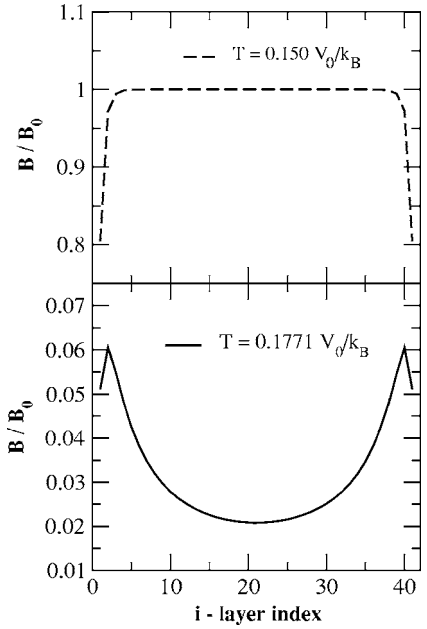

FIG. 4. Normalized compressibility elastic constant versus layer index for films at distinct temperatures. The parameters are the same as in Fig. 3. Notice that the compressibility elastic constant profile changes its curvature from negative to positive close to the transition temperature.

$$\Delta(T) = \frac{1}{16\pi}\sum_{n=1}^{\infty}\left(\frac{\gamma_c - \gamma}{\gamma_c + \gamma}\right)^{2n}\frac{1}{n^2}, \tag{15}$$

where $\lambda_c = \sqrt{K/B}$ is a characteristic length scale of the film. From Eq. (14), we can notice that an additional temperature dependence of the smectic Casimir-like force can appear from the temperature dependence of K and B in the expressions of γ_c and λ_c, as well as from their nonuniformity through the film. The above expression will be used to compare the fluctuation-induced force computed in the present work with that predicted by the continuous model of a uniform film. In this case, the temperature dependence of the coupling constants will be assumed to be derived from the mean-field model for bulk smectic LC.

In what follows, we analyze the behavior of the Casimir-like force for films with nonuniform elastic constant profiles. The results were numerically obtained from Eq. (8). First, we considered the case of a first-order SmA-N transition with $\alpha=0.85$, $\gamma=30$ dyn/cm, $d=30$ Å, $a=4$ Å, and $L=1$ cm. In Fig. 5, we plot the Casimir-like force as a function of temperature for different film thicknesses. For thick films, this effective long-range force exhibits only a small deviation from the result of the continuous model, as one approaches the bulk transition point. In contrast, the amplitude of this force in thin films increases significantly, with its magnitude being three orders of magnitude larger than that predicted when assuming uniform elastic constant profiles. This substantial increase of the Casimir-like force is directly related to the nonuniformity of the elastic constant profile in the central part of the film.

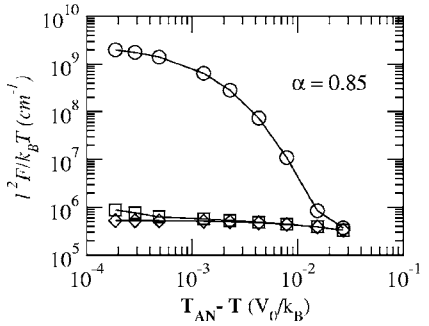

FIG. 5. $\ell^2(F/k_BT)$ versus reduced temperature for films with different thickness. The elastic constants were numerically obtained from the extended mean-field model [24,25] with the same parameters as in Fig. 1. The surface tension is $\gamma=30$ dyn/cm. The reference temperature was taken as $T_0=0.180V_0/k_B$. Circles stand for a film with 11 layers and squares are for a film with 41 layers. Diamonds represent the values predicted by Eqs. (14) and (15).

In Fig. 6, we plot the Casimir-like force as a function of temperature in the vicinity of the second-order SmA-N bulk transition ($\alpha=0.6$). In this case, the fluctuation-induced force is enhanced for both thick and thin films as the temperature is tuned closer to the bulk transition temperature. This feature reflects the nonuniformity of the elastic constant B close to the transition even for thick films. For thin films the amplitude displays a minimum which is a consequence of the competitive roles played by the nonuniformity of the profile and the vanishing of the elastic constant. For the second-order SmA-N phase transition, the translational order parameters σ_i vanish continuously when the temperature approaches to the bulk transition temperature. Therefore, the thermal Casimir force should decrease when the temperature increases. Whenever the profile at the film center remains flat, this is the predominant effect. As the profiles of the order parameters become sufficiently nonuniform at the film center, the amplitude tends to increase. Therefore, the competition between the vanishing of the order parameters and the development of a nonuniform profile results in a minimum of the Casimir-like force. For thick films, the nonuniformity is always predominant. The amplitude of the

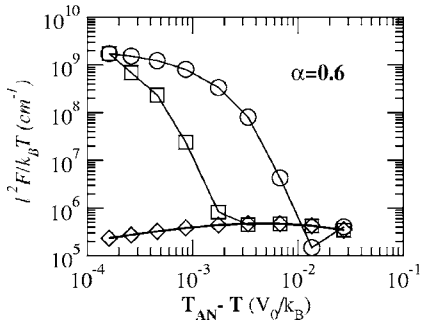

FIG. 6. $\ell^2(F/k_BT)$ versus reduced temperature for films with different thicknesses. The microscopic parameters are the same as in Fig. 3. The reference temperature was taken as $T_0=0.150V_0/k_B$. The circles represent data for a film with 11 layers and squares represent data for a 41 layer film. Diamonds are values predicted by Eqs. (14) and (15).

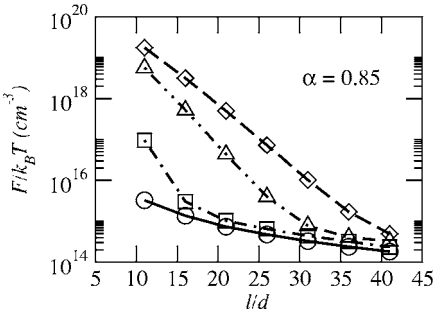

FIG. 7. The Casimir-like force versus film thickness for different temperatures, near a first-order transition. The microscopic parameters are the same of Fig. 1. The surface tension is $\gamma = 30$ dyn/cm and the temperatures are $T=0.180V_0/k_B$ (circles), $0.1991V_0/k_B$ (squares), $0.2057V_0/k_B$ (triangles), and $0.2068V_0/k_B$ (diamonds).

fluctuation-induced force also increases about three orders of magnitude near the transition temperature. These results show that the Casimir-like force can predominate over the van der Waals force in the vicinity of the Sm*A*-*N* transition temperature.

As shown above, the long-range interaction induced by smectic fluctuations presents distinct behaviors for thin and thick films close to the Sm*A*-*N* phase transition. This feature indicates that the order parameter profiles influence the thickness functional dependence of this force. In Fig. 7, we show the Casimir-like force as a function of the film thickness at different temperatures for $\alpha=0.85$. In all cases, we can notice that there is a crossover between distinct decays of the thermal Casimir-like force. The deviation from the predicted by Eq. (14) becomes more pronounced as the temperature approaches the Sm*A*-*N* transition point. In fact, for temperatures very close to the transition temperature the order parameter profiles are nonuniform even for thick films. Considering $\alpha=0.6$ and temperatures not very close to the transition temperature, the decay of the fluctuation-induced force has the same behavior as that exhibited near the first-order transition, as shown in Fig. 8(a). Close to the transition temperature, the Casimir-like force decays with thickness as $1/\ell^{3/2}$ for thin films.

This exponent can be also analytically supported by the divergence of the correlation length in the vicinity of the second-order smectic-nematic transition. In the regime of very thin films, the asymptotic expansion leading to a $1/\ell$ decay of the Casimir-like energy does not hold, and its main singular behavior is due to the vanishing of the compressional mode B [$\Delta f(\ell) \propto 1/\lambda_c \propto B^{1/2}$]. According to scaling arguments, the compressional mode is proportional to the inverse of the correlation length and therefore $\Delta f(\ell) \propto \xi^{-1/2}$ [1,2]. For thin films close to a second-order transition, the correlation length is limited by the film thickness ℓ, resulting in $\Delta f(\ell) \propto \ell^{-1/2}$, thus supporting our extrapolated exponent for the Casimir-like force $F(\ell) \propto \ell^{-3/2}$.

IV. SUMMARY AND CONCLUSIONS

In this work, using a Gaussian functional integral approach, we studied the effects of order parameter profiles on

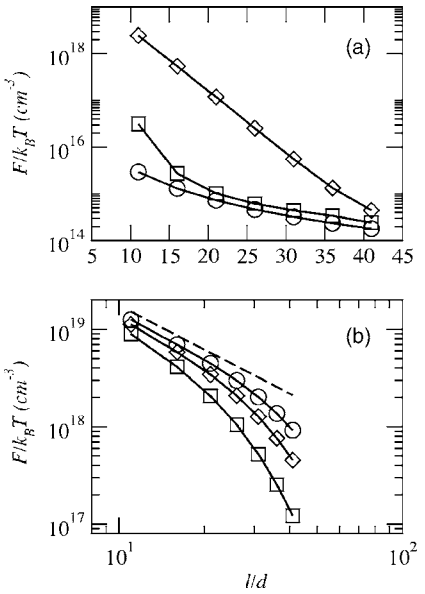

FIG. 8. The Casimir-like force versus film thickness for different temperatures, close to the second-order transition. The microscopic parameters are the same as in Fig. 3. The surface tension is the same as in Fig. 5. The temperatures are (a) $T=0.150V_0/k_B$ (circles), $0.1705V_0/k_B$ (squares) and $0.1755V_0/k_B$ (diamonds); (b) $T=0.1768V_0/k_B$ (squares), $0.1770V_0/k_B$ (diamonds), and $0.1771V_0/k_B$ (circles). The dashed line represents a decay in the form $1/\ell^{3/2}$.

the Casimir-like force in free-standing smectic-*A* films. The profiles of order parameters were numerically calculated from the microscopic theory [24,25] and associated with the hydrodynamical Hamiltonian through the elastic constants of each film layer. It was shown that the amplitude of the thermal Casimir-like force has a strong dependence on the order parameter profiles close to first- and second-order smectic-*A*–nematic transition temperatures. In both cases, the amplitude of the fluctuation-induced force increases for several orders of magnitude, indicating that the thermal Casimir contribution due to fluctuations of the smectic order predominates over the van der Waals force in these systems. Further, the nonuniformity of the elastic constant profiles close to the transition temperature modifies the functional dependence of fluctuation-induced long-range force on the film thickness ℓ. In the vicinity of the second-order smectic-*A*–nematic phase transition point, the force decays as $1/\ell^{3/2}$ in contrast to the $1/\ell^2$ decay far from the bulk transition temperature. This feature is due to the divergence of the typical correlation length which also governs the vanishing of the compressional elastic constant. Although higher-order fluctuations may imply in corrections to the above scaling, especially at the vicinity of continuous transitions at which fluctuations grow unbounded, the present results consistently show that the thermal fluctuation-induced force is indeed the predominant long-range interaction for temperatures slightly below the bulk Sm*A*-*N* phase transition. Previous experimental measurements, based on the relation between the surface interaction and the contact angle with the film meniscus, have indeed shown a relative increase of the surface interaction as

the bulk smectic-*A*–nematic transition temperature is approached from below [38]. Once more precise experimental techniques are nowadays available [39], the presently predicted scaling behavior can be probed and corrections to the Gaussian behavior estimated.

ACKNOWLEDGMENTS

We would like to thank CAPES, CNPq, and FINEP (Brazilian Research Agencies) as well as FAPEAL (Alagoas State Research Agency) for partial financial support.

[1] P. G. de Gennes and J. Prost, *The Physics of Liquid Crystals* (Clarendon Press, Oxford, 1993).
[2] S. Chandrasekhar, *Liquid Crystals* (Cambridge University Press, Cambridge, U.K., 1992).
[3] C. Rosenblatt and N. M. Amer, Appl. Phys. Lett. **36**, 432 (1980).
[4] S. Heinekamp, R. A. Pelcovits, E. Fontes, E. Y. Chen, R. Pindak, and R. B. Meyer, Phys. Rev. Lett. **52**, 1017 (1984).
[5] C. Bahr, Int. J. Mod. Phys. B **8**, 3051 (1994).
[6] T. Stoebe, P. Mach, and C. C. Huang, Phys. Rev. Lett. **73**, 1384 (1994).
[7] E. I. Demikhov, V. K. Dolganov, and K. P. Meletov, Phys. Rev. E **52**, R1285 (1995).
[8] L. V. Mikheev, Zh. Eksp. Teor. Fiz. **96**, 632 (1989) [Sov. Phys. JETP **69**, 358 (1989)].
[9] A. Ajdari, L. Peliti, and J. Prost, Phys. Rev. Lett. **66**, 1481 (1991).
[10] H. Li and M. Kardar, Phys. Rev. Lett. **67**, 3275 (1991).
[11] M. L. Lyra, M. Kardar, and N. F. Svaiter, Phys. Rev. E **47**, 3456 (1993).
[12] B. D. Swanson and L. B. Sorensen, Phys. Rev. Lett. **75**, 3293 (1995).
[13] P. Ziherl, R. Podgornik, and S. Zumer, Phys. Rev. Lett. **84**, 1228 (2000).
[14] P. Ziherl, F. Karimi Pour Haddadan, R. Podgornik, and S. Zumer, Phys. Rev. E **61**, 5361 (2000).
[15] E. A. L. Mol, G. C. L. Wong, J. M. Petit, F. Rieutord, and W. H. de Jeu, Physica B **248**, 191 (1998).
[16] E. A. L. Mol, G. C. L. Wong, J. M. Petit, F. Rieutord, and W. H. de Jeu, Phys. Rev. Lett. **79**, 3439 (1997).
[17] R. Lucht, P. Marczuk, Ch. Bahr, and G. H. Findenegg, Phys. Rev. E **63**, 041704 (2001).
[18] J. Als-Nielsen, F. Christensen, and P. S. Pershan, Phys. Rev. Lett. **48**, 1107 (1982).
[19] A. Fera, B. I. Ostrovskii, D. Sentenac, I. Samoilenko, and W. H. de Jeu, Phys. Rev. E **60**, R5033 (1999).
[20] I. N. de Oliveira and M. L. Lyra, Phys. Rev. E **65**, 051711 (2002).
[21] I. N. de Oliveira and M. L. Lyra, Phys. Rev. E **70**, 050702(R) (2004).
[22] R. Holyst, D. J. Tweet, and L. B. Sorensen, Phys. Rev. Lett. **65**, 2153 (1990).
[23] R. Holyst, Phys. Rev. A **44**, 3692 (1991).
[24] L. V. Mirantsev, Phys. Lett. A **205**, 412 (1995).
[25] L. V. Mirantsev, Liq. Cryst. **20**, 417 (1996).
[26] P. Ziherl, Phys. Rev. E **61**, 4636 (2000).
[27] N. Uchida, Phys. Rev. Lett. **87**, 216101 (2001).
[28] L. V. Mirantsev, Phys. Solid State **41**, 1729 (1999).
[29] L. V. Mirantsev, Phys. Rev. E **62**, 647 (2000).
[30] J. Collett, L. B. Sorensen, P. S. Pershan, and J. Als-Nielsen, Phys. Rev. A **32**, 1036 (1985).
[31] R. Jaquet and F. Schneider, Phys. Rev. E **67**, 021707 (2003).
[32] M. Veum, P. Messman, Z. Q. Liu, C. C. Huang, N. Janarthanan, and C. S. Hsu, Rev. Sci. Instrum. **74**, 5151 (2002).
[33] M. Veum, E. Kutschera, N. Voshell, S. T. Wang, S. L. Wang, H. T. Nguyen, and C. C. Huang, Phys. Rev. E **71**, 020701(R) (2005).
[34] T. Stoebe, P. Mach, S. Grantz, and C. C. Huang, Phys. Rev. E **53**, R1662 (1996).
[35] P. Mach, C. C. Huang, T. Stoebe, E. D. Wedell, T. Nguyen, W. H. de Jeu, F. Guittard, J. Naciri, R. Shashidhar, N. Clark, I. M. Jiang, F. J. Kao, H. Liu, and H. Nohira, Langmuir **14**, 4330 (1998).
[36] W. L. McMillan, Phys. Rev. A **4**, 1238 (1971).
[37] W. H. de Jeu, B. I. Ostrovskii, and A. N. Salaginov, Rev. Mod. Phys. **75**, 181 (2003).
[38] F. Picano, P. Oswald, and E. Kats, Phys. Rev. E **63**, 021705 (2001).
[39] P. V. Dolganov, P. Cluzeau, G. Joly, V. K. Dolganov, and H. T. Nguyen, Phys. Rev. E **72**, 031713(R) (2005).